# Application of AFM on the Adhesion Studies of Oxygen-Plasma-Treated Polypropylene and Lignocellulosics

R. Mahlberg*

*VTT Building Technology, Wood Technology, P.O. Box 1806, FIN-02044 VTT, Finland*

H. E.-M. Niemi

*Laboratory of Physics, Helsinki University of Technology, P.O. Box 1100, FIN-02015 HUT, Finland*

F. S. Denes

*Engineering Research Center for Plasma-Aided Manufacturing, University of Wisconsin, Madison, Wisconsin 53706*

R. M. Rowell

*Forest Products Laboratory, USDA Forest Service, One Gifford Pinchot Drive, Madison, Wisconsin 53705-2398*

*Received February 5, 1998. In Final Form: December 31, 1998*

Atomic force microscopy was used to study the surfaces of oxygen-plasma-treated polypropylene (PP), kraft pulp, filter paper, and wood. The effect of plasma treatment on the adhesion properties between PP film and wood was evaluated by means of a peel test. The highest adhesion to wood resulted from the shortest treatment times used. The effects of plasma on the adhesion properties were more pronounced when both the PP film and the wood surface were treated. Oxygen plasma caused changes in the morphology of the materials: the treated PP surface was covered by a nodular structure, which was not seen on the untreated film. A similar nodular structure was also seen on the lignocellulosic materials. These nodules seemed to have poor interaction with the PP surface, resulting in a weak interface between the plastic film and wood.

## Introduction

In composites made from lignocellulosic and thermoplastic materials, incompatibility between the components often causes problems in the processing and utilization of the composites. The incompatibility problems between the hydrophilic lignocellulosic material and the hydrophobic thermoplastics can be overcome by improving the adhesion using compatibilizers or coupling agents. In the paper, electronics, and textile industries, research has focused mainly on modification of surfaces with plasma, corona, or flame treatments.[1–3] The use of plasma for pretreating polymers in order to enhance their adhesion has been known for over 20 years.[4,5] Cold plasmas affect the top layers of a surface and do not cause any changes in the bulk properties of the material. Plasma treatments are known to form polymer radicals on the treated surfaces, which react with oxygen when exposed to air after treatment. The polarity of the surfaces increases due to the polar groups formed.

A better understanding of the chemical and physical effects of plasma treatments on cellulosic and synthetic materials is required before the technique can be applied commercially. The ultimate objective of this study was to improve the adhesion between a polypropylene film and wood substrate by plasma treatment and to increase our knowledge of the fundamental phenomena taking place in the modification. As simple model materials for lignocellulosics, kraft pulp and filter paper (cellulose) were used to study the effects of the modification. However, the information related to cellulose may be expanded to wood/thermoplastic composites as well.

Adhesion between two surfaces has been suggested to be a result of an interaction of two factors: an intimate molecular contact and a maximum attractive force between the components.[6,7] The concept of intimate molecular contact consists of the following theories: adsorption, diffusion, interlocking, and weak boundary. The maximum attractive force theories involve the theories of chemical bonding, acid-base, electrostatic, and again weak boundary layer. While the adsorption theory is based on the rules of spreading and wetting, the diffusion and interlocking theories explain adhesion through physical contact (entanglements) and through interpenetration (anchoring), respectively. In general, these theories deal with the fact that two surfaces have to come into sufficient contact with each other so that the premises for attractive forces are met. The chemical bonding theory explains that the covalent, hydrogen, van der Waals, ionic, and metallic bonds are responsible for adhesion. In the electrostatic

(1) Westerlind, B.; Larsson, A.; Righdal, M. *Int. J. Adhesion Adhesives* **1984,** *3,* 141.
(2) Gerenser, L.; Ehnan, J.; Mason, M.; Pochan, J. *Polymer* **1985,** *26,* 1162.
(3) Briggs, D.; Kendall, C. R. *Int. J. Adhesion Adhesives* **1982,** *2,* 13.
(4) Hall, J. R.; Westerdahl, C. A. L.; Devine, A. T.; Bodnar, M. J. *J. Appl. Polym. Sci.* **1969,** *13,* 2085.
(5) Kaelble, D. H.; Dynes, P. J.; Cirlin, E. H. *J. Adhesion* **1974,** *6,* 23.
(6) Chung, F. H. J. *J. Appl. Polym. Sci.* **1991,** *42,* 1319.
(7) Marian, J. E.; Stumbo, D. A. *Holzforschung* **1962,** *5,* 134.

10.1021/la980139b CCC: $18.00 
Published on Web 03/19/1999

theory, adhesion derives from the electrostatic effects at the interface. In the acid-base theory, hydrogen bonding is the key to adhesion. Instead of explaining why two materials stick together, the weak boundary theory explains what makes adhesion fail. Lack of molecular contact and weak intermolecular attraction results in a weak boundary layer which acts as a rupture center and leads to failure in adhesion.[6]

The present paper focuses on the surface morphology of polypropylene (PP) film and the lignocellulosic materials mentioned above. Correlations between the adhesion and the morphology of oxygen-plasma-treated PP films and wood were also investigated. The morphological features of the surfaces were studied using atomic force microscopy (AFM), which is a suitable tool for observing the changes in morphology on the nanoscale. A standard peel test was used for the adhesion studies.

The AFM measurements were made using the tapping mode developed especially for studying soft and fragile samples. The invention of the tapping mode in atomic force microscopy has overcome the problems of traditional contact mode imaging, such as modifying the surface, friction, adhesion, and electrostatic forces. Instead of dragging the tip across the surface as in the conventional contact mode, tapping mode imaging is done by oscillating the cantilever within a frequency of few hundred kilohertz near its resonance, using an amplitude normally over 20 nm. The oscillation and the force on the sample are maintained constant by a feedback loop. The tip is brought close to the surface until it begins to touch the surface by tapping it gently, which reduces the oscillation amplitude. While scanning the surface, the amplitude alternates depending on the topography, increasing when there is a depression and decreasing above a bump. Information is collected from the changes in amplitude. No lateral, shear, or friction force is applied to the sample and no sticking occurs, since the tip contacts the surface briefly during each oscillation. Therefore, tapping mode imaging has made it possible to study samples that are easily damaged or loosely bound to the substrate. Plasma-modified materials with minor changes fall into this category.

In recent years, the application of AFM to surface morphology studies of polymers has grown rapidly. It has already been used to study polyethylene,[9] polypropylene,[10] polyaniline,[11,12] polypyrrole,[13,14] methyl methacrylate,[15] crystallized or polymerized *in situ*, and nylon[16] films, to mention a few. Several studies on oxygen-plasma-treated polymer films have been conducted, for example, on the following: polypropylene,[17–19] poly(tetrafluoroethylene) (PTFE),[20] and polyimide film.[21] Besides oxygen plasma, the AFM technique has been applied to study the effects of many other types of plasma treatments, such as He, Ar, Xe, $N_2$, $H_2$, and $NH_3$.[17,18,20–22] In addition, AFM studies on the effects of other surface modification methods, such as corona treatments,[23,24] have shown the capability of AFM to provide new information on the minor changes, especially, at the nanometer level for the first time.

## Experimental Section

**Materials.** The nonoriented, two-layered polypropylene-polyamide film was supplied by Walki Pack Valkeakoski (Finland). The polypropylene (PP) layer had a thickness of 50 $\mu$m and the polyamide (PA) layer 30 $\mu$m. The PP film reinforced with a PA layer was used in order to be able to peel the thin film off the substrate without breaking it. Prior to the plasma treatments, the plastic films were cut into the shape and size of the plasma electrode and washed several times with acetone (Soxhlet extractions).

Sliced birch (*Betula pendula*) and spruce (*Picea abies*) veneer of 0.8-mm nominal thickness (radial direction) were used as the substrates for PP/PA films. The size of the veneer samples used for the plasma treatments was 60 mm × 170 mm (tangential × longitudinal, respectively). Prior to the plasma treatments, the veneer surfaces were smoothed by sanding them with a sand paper of 150 grid followed by Soxhlet extraction of the veneer panels with acetone. After the extractions, the veneer samples were oven-dried for 20 h at 105 °C. Filter paper (rich in cellulose; Schleicher & Schuell) and kraft pulp with a $\kappa$ number of 123 and originating from loblolly pine served as the model materials of wood veneer for the morphology studies.

**Plasma Installation.** Oxygen plasma treatments were carried out using a plasma installation from the Engineering Research Center for Plasma-Aided Manufacturing of the University of Wisconsin (Madison). All plasma treatments of the natural and synthetic polymeric substrate surfaces were carried out in a cylinderical, capacitively coupled, parallel-plate, 50-kHz RF plasma reactor made of stainless steel and provided with thermostating possibilities (25–500 °C) of the electrodes. Plasma treatments were preceded by cleaning procedures of the reactor in order to avoid possible contamination of the substrates from the reactor wall originating from previous experiments. The decontamination method involved heating the substrate holder electrode (lower electrode) to 200 °C, introducing oxygen plasma (230 mTorr; 200 W, 10 min) followed by argon plasma under similar conditions, and cooling the electrode and promoting the plasma reactor to the low-pressure level.

**Plasma Treatments.** In a typical experiment, after the reactor was decontaminated, the selected two identical substrates were positioned on the lower electrode, the chamber was then closed, and a low pressure was created in the system. In the next step, oxygen was introduced into the reactor under the preselected pressure and flow-rate conditions. The RF plasma was then ignited, and the discharge was sustained for the desired power and treatment time values. At the end of the reaction, the RF power was disconnected, and the base pressure was restored in the system. The reactor was then repressurized by introducing air, and the samples were removed and stored under vacuum desiccator conditions until starting the analytical evaluations.

The following experimental conditions were employed during the plasma treatments: base pressure, 50 mT, pressure of $O_2$ in the absence of plasma, 200 mTorr; pressure of $O_2$ in the presence of plasma, 225–280 mTorr; RF power dissipated to the electrodes, 100 W; flow rate of $O_2$, 6.5 sccm; reaction time, 15, 30, 45, 60, 75, and 90 s.

**Scanning Electron Microscopy (SEM).** The plasma-treated sample surfaces were vacuum coated by evaporation with gold and examined by means of a JEOL JSM-840 and a JEOL JSM-820 scanning electron microscopes. The accelerating voltages

(8) Digital Instruments Inc.
(9) Magonov, S. N.: Sheiko, S. S.; Deblieck, R. A. C.; Möller, M. *Macromolecules* **1993,** *26,* 1380.
(10) Stocker, W.; Bickmann, B.; Magonov, S. N.; Cantow, H.-J.; Lots, B.; Wittmann, J.-C.; Möller, M. *Ultramicr.* **1992,** *42–44,* 1141.
(11) Kugler, T.; Rasmusson, J. R.; Österholm, J.-E.; Monkman, A. P.; Salaneck, W. R. *Synth. Met.* **1996,** *76,* 181.
(12) Porter, T. L.; Sykes, A. G.; Caple, G. *Surf: Int. Anal.* **1994,** *21,* 814.
(13) Li, J.; Wang, E. *Synth. Met.* **1994,** *66,* 67.
(14) Li, J.; Wang, E.; Green, M.; West, P. E. *Synth. Met.* **1995,** *74,* 127.
(15) Li, G.; Tobin, J. A.; Denton, D. D. *Appl. Phys. Lett.* **1994,** *64,* 560.
(16) Zhang, J.; Watson, B. A.; Keown, R. W.; Malone, C. P.; Barteau, M. A. *Langmuir* **1995,** *11,* 3018.
(17) Colland, M.; Groening, P.; Nowak, S.; Schlapbach, L. *J. Adhesion Sci. Technol.* **1994,** *8,* 1115.
(18) Collaud Coen, M.; Dietler, G.; Kasas, S.; Gröning, P. *Appl. Surf Sci.* **1996,** *103,* 27.
(19) Gross, T.; Lippitz, A.; Unger, W. E. S.; Friedrich, J. F.; Wöll, C. *Polymer* **1994,** *35,* 5590.
(20) Ryan, M. E.; Badyal, J. P. S. *Macromolecules* **1995,** *28,* 1377.
(21) Inagaki, N.; Tasaka, S.; Hibi, K. *J. Adhesion Sci. Technol.* **1994,** *8,* 395.
(22) Gengenbach, T. R.; Xie, X.; Chatelier, R. C.; Griesser, H. J. *J. Adhesion Sci. Technol.* **1994,** *8,* 305.
(23) Overney, R. M.; Lüthi, R.; Haefke, H.; Frommer, J.; Meyer, E.; Güntherodt, H.-J. *Appl. Surf. Sci.* **1993,** *64,* 197.
(24) Overney, R. M.; Güntherodt, H.-J.; Hild, S. *J. Appl. Phys.* **1994,** *75,* 1401.

**Table 1. Effect of Oxygen Plasma Treatment on the Peel Strength between Wood and PP**

| specimen | treatment conditions: time, s | power, W | pressure, mTorr | bonding strength, N/mm: max | min | wood failure, % |
|---|---|---|---|---|---|---|
| **Spruce** | | | | | | |
| 1. untreated spruce + untreated PP | | | | 0.20 ± 0.02 | 0.12 ± 0.02 | ≤10 |
| 2. untreated spruce + treated PP | 15 | 100 | 200−225 | 0.22 ± 0.05 | 0.16 ± 0.03 | 30− 40 |
| 3. treated spruce + | 15 | 100 | 200−250 | 0.27 ± 0.03 | 0.20 ± 0.04 | 40−100 |
| treated PP | 15 | 100 | 200−225 | | | |
| 4. untreated spruce + treated PP | 30 | 100 | 200−225 | 0.20 ± 0.11 | 0.13 ± 0.12 | 10−40 |
| 5. treated spruce + | 30 | 100 | 200−250 | 0.22 ± 0.03 | 0.14 ± 0.03 | 30−100 |
| treated PP | 30 | 100 | 200−225 | | | |
| 6. untreated spruce + treated PP | 60 | 100 | 200−225 | 0.22 ± 0.06 | 0.18 ± 0.07 | 20−30 |
| 7. treated spruce + | 60 | 100 | 200−250 | 0.24 ± 0.03 | 0.19 ± 0.03 | 20−40 |
| treated PP | 60 | 100 | 200−225 | | | |
| **Birch** | | | | | | |
| 1. untreated birch + untreated PP | | | | 0.21 ± 0.02 | 0.13 ± 0.05 | ≤10 |
| 2. treated birch + | 15 | 100 | 200−250 | 0.41 ± 0.02 | 0.29 ± 0.02 | 30−70 |
| treated PP | 15 | 100 | 200−225 | | | |
| 3. treated birch + | 30 | 100 | 200−250 | 0.23 ± 0.03 | 0.19 ± 0.06 | 20−40 |
| treated PP | 30 | 100 | 200−225 | | | |
| 4. treated birch + | 60 | 100 | 200−250 | 0.29 ± 0.02 | 0.22 ± 0.04 | 20−50 |
| treated PP | 60 | 100 | 200−225 | | | |

used in the SEM analyses varied from 1 to 15 kV depending on the level of intended resolution.

**Atomic Force Microscopy (AFM).** The AFM measurements were carried out at ambient pressure, room temperature, and room humidity, using a multimode NanoScope III[9] instrument. The noncontact tapping mode was used for taking topographic images. The resonant oscillating frequencies were around 320 kHz, and the scanning rates varied from 0.4 to 2.5 Hz, depending on the size of the scan area. A 200 $\mu$m scanner and commercial etched silicon tips[8] were employed during the morphology evaluations. The quality of the tips was checked before and after the measurements with a reference sample consisting of small, round-shaped quantum dots (InP/GaAs[25]). The mean spring constant of the tips was 36 N/m, the length was 125 $\mu$m, and the tip ends were about 10 nm in diameter. The samples were attached to the sample holder with double-sided tape. Repeatable images of the plasma-treated polypropylene films and paper were taken using different tips. The different. plasma-treated samples were measured both with the same tip and with different tips in order to be able to compare the results.

The images are mainly raw data except that in some cases, minor flatness and tilt corrections have been made. The rms (root-mean-square) surface roughness was determined as the standard deviation of $Z$ values within the given area and calculated using the following equation:

$$R_{rms} = R(F\sum(Z_i - Z_{ave})^2, N)$$

where $Z_{ave}$ is the average of the $Z$ values within the given area, $Z_i$ is the current $Z$ value, and $N$ is the number of points within the given area. Each surface roughness value presented has been averaged from seven separate measurements from different areas, and the error has been estimated as a standard deviation.

**Sample Preparations and Peel Test.** The adhesion strength of the PP to wood surface was tested using a 90° peel test. This test was slightly modified from the standard test of ASTM D 3167-76.[26] The width of the test specimens (25.4 mm) used in this study differed from the one (12.7 mm) of the standard in order to narrow down the edge effect resulting from possible stresses and damage at the edges of the test specimens during the cutting of the specimens. The specimens for the peel test were prepared as follows:

(1) The plasma-treated veneer panels and control panels (dried in a vacuum oven) were coated with the PP/PA film (PP facing the wood surface) using a laboratory-scale press. A pressure of 2.7 MPa, a pressing time of 3 min, and a temperature of 150 ± 5 °C were applied during the procedure. A cooling period down to 50 °C under pressure followed the hot pressing.

(2) The laminated panels were cut into strips with dimensions of 25.4 mm × 170 mm, discarding the edges of the panels.

(3) The peel test specimens were then conditioned at 65% relative humidity (FLH) and 26.6 °C before carrying out the peel tests.

## Results

**Peel Strength Measurements.** To determine the effect of plasma treatment on the adhesion between PP film and wood, adhesion specimens were made by coating wood veneer (untreated/treated birch and spruce) with PP film (untreated/treated). The lengths of the treatment times for the substrate and the coating were 15, 30, and 60 s.

The peel test results for different combinations of laminated specimens are shown in Table 1. The results are the mean values of 12 measurements derived from 3 replica treatments. The wood failure percentages are evaluated by the naked eye. The peel test results show that the lowest bonding strength values are given by the control specimens (untreated wood laminates with untreated PP). The percentage of wood failure on the fracture surface of the control specimens was less than or equal to 10%, which was significantly lower than the wood failure values of the treated specimens. The highest adhesion values were observed for the specimens with the shortest treatment time (15 s). This trend was noted for both wood species, even though the effect of plasma treatment was more pronounced in the case of birch. Increased wood failure values, together with higher bonding strength, indicate that improvement of adhesion due to plasma has taken place. The adhesion is improved slightly more, when both the substrate and the film surfaces are treated, as compared with the specimens in which only the plastic film was treated.

**Atomic Force Microscopy Analyses. The** morphological changes on polypropylene and kraft pulp were studied with AFM as a function of treatment time. In addition, the differences in morphological changes were compared between kraft pulp and filter paper. A wood sample with a long treatment time (90 s) was also imaged. Table 2 shows the treatment times for the different materials.

**Polypropylene.** Figure 1 shows a typical, large-scale AFM image (50 $\mu$m × 50 $\mu$m) of the PP film surface that

(25) Ahopelto, J.; Lipsanen, H.; Sopanen, M.; Koljonen, T.; Niemi, H. E.-M. *Appl. Phys. Lett.* **1994,** *65,* 1662.

(26) ASTM D 3167-76, Standard test method for floating roller peel resistance of adhesives.

**Table 2. Treatment Times for the Samples Imaged with AFM[a]**

| sample | treatment time, s | | | | | | |
|---|---|---|---|---|---|---|---|
| | $t_1$ | $t_2$ | $t_3$ | $t_4$ | $t_5$ | $t_6$ | $t_7$ |
| PP | 0 | | 30 | 45 | 60 | 75 | |
| kraft pulp | 0 | 15 | 30 | | 60 | | 90 |
| filter paper | 0 | | 30 | | 60 | | |
| wood | 0 | | | | | | 90 |

[a] The treatment conditions kept constant were the following: power, 100 W; pressure, 200 mTorr; gas flow rate, 6.5 sccm.

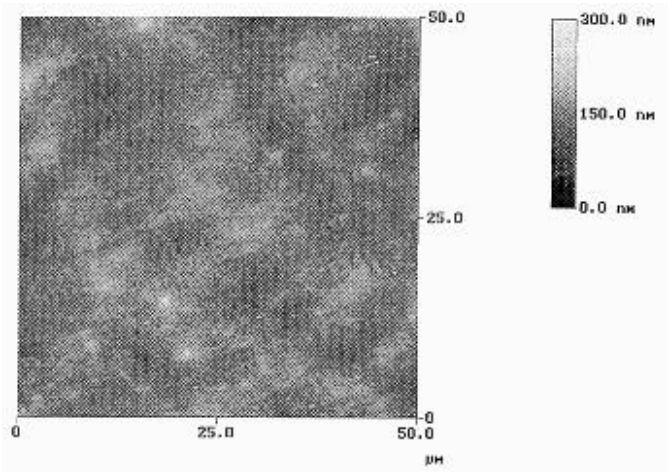


**Figure 1.** AFM image (50 $\mu$m × 50 $\mu$m) of the polypropylene surface modified with oxygen plasma for 60 s. The hollows and veins caused by manufacturing processes are shown on the surface.

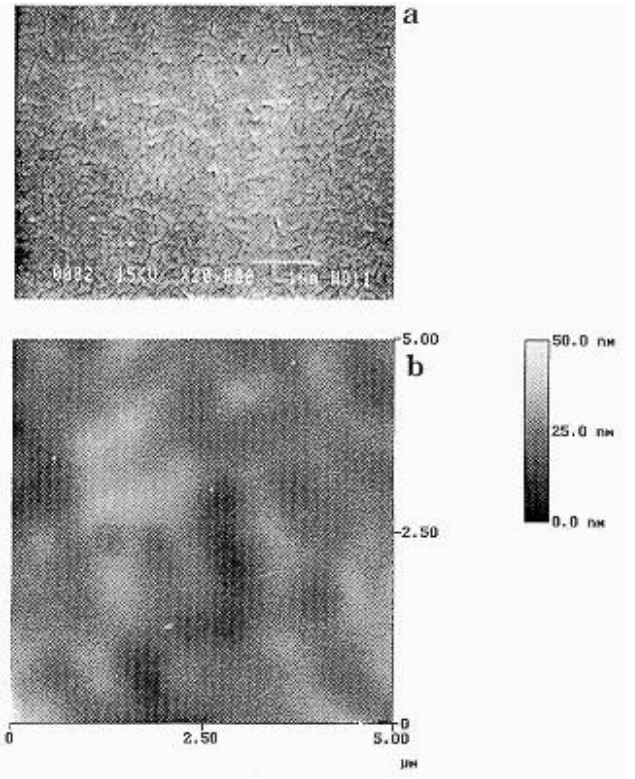


**Figure 2.** Plasma-treated (60-s) polypropylene surface imaged by (a) SEM and (b) AFM techniques (both 5 $\mu$m × 5 $\mu$m). The SEM micrograph is covered by a cracklike pattern which is not seen in the AFM image.

has been oxygen plasma treated for 60 s. The film surface is granular with no regular structure; the surface is uneven and the roughness is about 20 ± 1 nm. Small holes and cracks are present as well as a slight orientation across the image which has presumingly been formed during the manufacturing of the film.

For evaluation of morphological changes due to plasma treatments of the material surfaces in addition to AFM analyses, the SEM technique at the magnification of 20 000× was used. To perform an accurate comparison between the SEM micrographs and AFM images of the same PP film surface, four measurements were made. First, the bare plasma-treated surface was imaged with AFM. Second, a thin gold layer was evaporated on the surface for SEM measurements and imaged with AFM before the SEM analysis. Finally, after taking the SEM micrographs, the sample was imaged once more with AFM.

The SEM micrographs revealed some deep and large cracks on the surface of the PP film that had been plasma treated for 60 s, as can be seen in Figure 2a. The untreated, as well as the oxygen-plasma-treated PP film, was covered with cracks, forming a netlike pattern on the surfaces. The pattern on the surfaces of the treated films looked the same, regardless of the length of the plasma treatments. In the corresponding AFM image of 5 $\mu$m × 5 $\mu$m (Figure 2b), there are no signs of cracks; instead, the surface seems to be quite smooth, consisting of hills and valleys. This suggests that the powers used in the SEM imaging may have damaged the surface. Because SEM microscopy does not give enough information on the film surface at the nanometer level, especially in the height direction, AFM imaging was used for studying the surfaces at this level.

An AFM image of untreated PP film cleaned by solvent extraction just before measurements is shown in Figure 3a. A spherulitic structure with clearly visible lamellae is observed. Otherwise, the untreated PP surfaces typically seem granular, quite smooth, but unhomogeneous. The mean roughness is about 3.0 ± 0.2 nm for an image of 1 $\mu$m × 1 $\mu$m. After the surface has been treated with plasma for 30 s, the surface gets slightly smoother as can be seen in Figure 3b. There is no significant change in the mean surface roughness value, but clear, roundish structures are visible, and some deep valleys can be observed. The PP film surface that had been plasma-treated for 45 s (Figure 3c) does not seem very different from the sample of 30 s. The roughness is slightly smaller and nodule size larger, and some valleys are still present.

A distinct change in the surface structure is observed after the surface has been treated with plasma for 60 s, as shown Figure 3d. The surface is smooth and consists of round-shaped features forming a nodular structure. The diameter of these features was found to be around 30 nm. The vertical heights measured from cross sections are of the order of 1–2 nm. The obtained surface roughness is about half that of the control film. After the PP film has been treated for 75 s, the diameter of the nodules increases, as can be seen in Figure 3e. On these surfaces, the diameter of the nodules is approximately 40–50 nm and the height varies from 4 to 6 nm. The surface is homogeneous, but the roughness is higher as compared with that of the 60-s sample, though it is less than that of the control sample.

Because the surface of the PP film is not homogeneous, the roughness values were estimated for each treatment time from four different image sizes (500 nm × 500 nm, 1 $\mu$m × 1 $\mu$m, 2 $\mu$m × 2 $\mu$m, and 5 $\mu$m × 5 $\mu$m) as shown in Figure 4. These values were determined as averages from several images taken from topographically similar areas free of manufacturing defects. The surface roughness is clearly dependent on the image size, but in each case, the trend is the same. The surface roughness values decrease slightly as the plasma treatment time increases

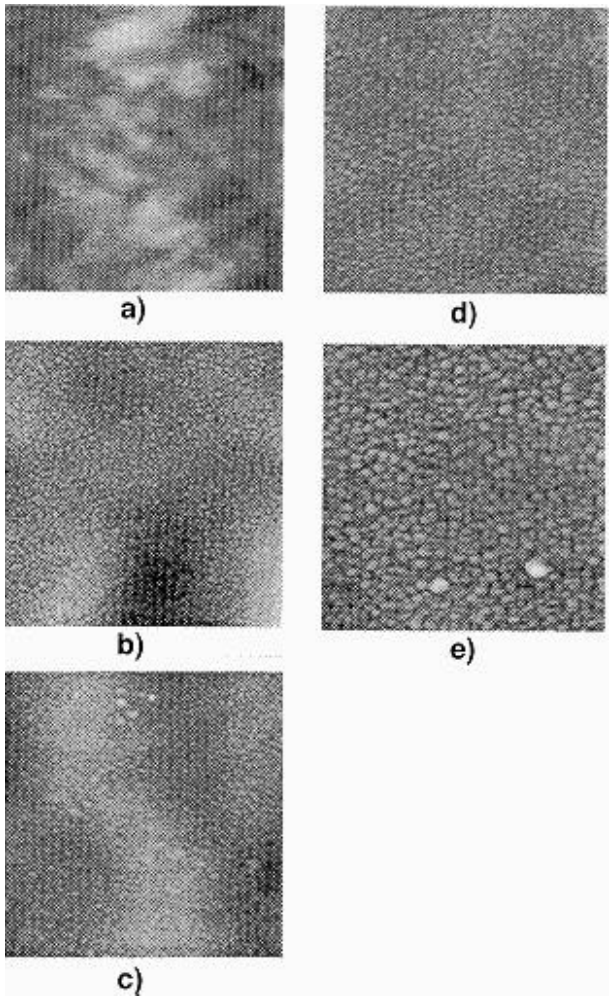


**Figure 3.** AFM images of the polypropylene surface treated with oxygen plasma for (a) 0, (b) 30, (c) 45, (d) 60, and (e) 75 s. The axis (1 $\mu$m × 1 $\mu$m) and depth (50 nm) scales are the same for all the images. While gradual formation of nodules on the treated surfaces is clearly observed, no nodule structure is seen on the untreated surface. The size of the nodules increases with the exposure time of plasma.

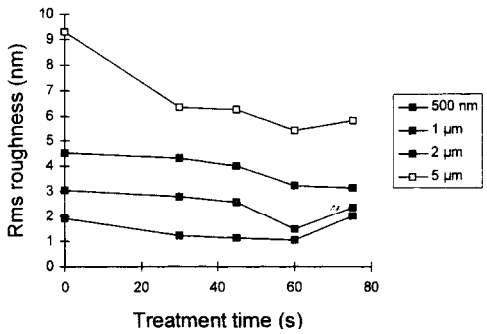


**Figure** 4. Effect of the plasma exposure time on the rms roughness of the polypropylene film at different levels of image size. Surface roughness decreases gradually with the exposure tune but is dependent on the image size.

until after 60 s the values start to increase. The surface roughness of 30-s oxygen-plasma-treated PP is comparable to the roughness of untreated PP film at the three smallest image sizes. When roughness comparisons are made using the image size of 5 $\mu$m × 5 $\mu$m, oxygen treatment for 30 s smooths the surface as compared with the untreated control film. The same kind of behavior was also observed in larger scale images (10 $\mu$m × 10 $\mu$m, 20 $\mu$m × 20 $\mu$m, 50 $\mu$m × 50 $\mu$m, and 100 $\mu$m × 100 $\mu$m). Further treatments

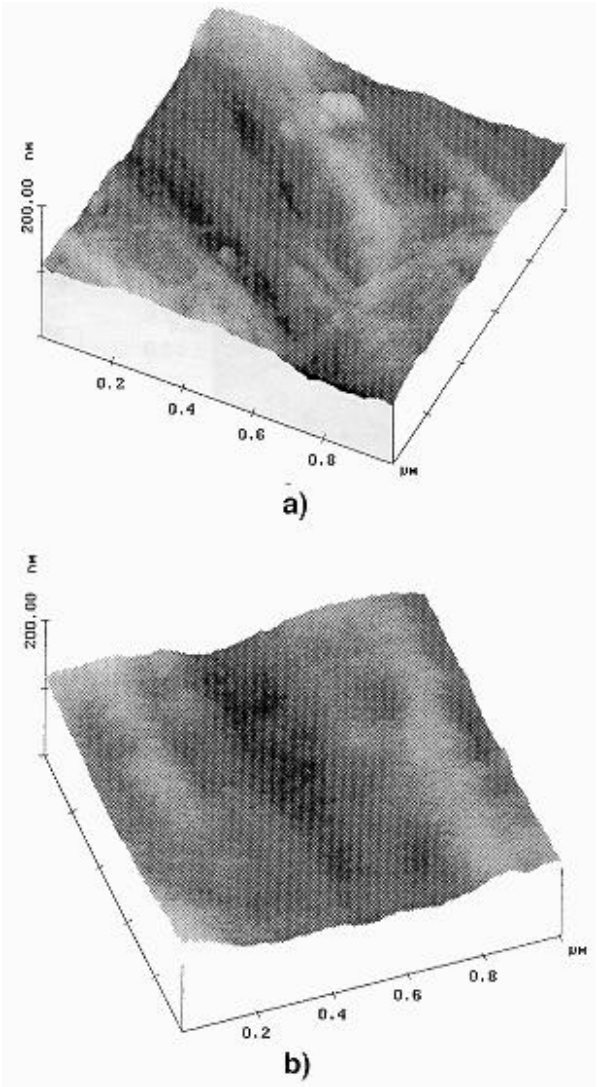


**Figure 5.** AFM image (1 $\mu$m × 1 $\mu$m) of (a) untreated birch surface and (b) birch surface treated with oxygen plasma for 90 s. Nodular structure caused by plasma treatment can be seen on the fiber surface.

for 45 and 60 s increase the smoothing effect slightly, and after that, the surface gets a bit rougher. The images of a smaller size present, rather, the influence of the nodule size on roughness.

**Lignocellulosic Materials.** The heterogeneous structure of the wood surfaces due to the open-cut fibers (and vessels in the case of birch), cross sections of ray cells, cell wall areas, out-sticking fragments of all these substances, etc., makes it difficult to prepare, by cutting or slicing, samples that are even enough for AFM measurements. From these specimens, it is hard to find smooth areas large enough to scan without destroying the tip. In addition, multitip images are common; occasionally part of the cantilever or tip gets stuck to a higher area in the sample, making the imaging impossible, and sometimes the tip is destroyed while approaching the surface. Therefore, it seemed reasonable to use other lignocellulosic materials, such as kraft pulp containing lignin, and filter paper without lignin, for simulating wood.

Despite the difficulties in using wood for AFM analyses, the imaging of wood surfaces was carried out to a certain extent. The AFM image of pine wood taken at the micrometer level, shown in Figure 5, demonstrates the effect of plasma treatment for 90 s. A similar nodular structure, noticed in all the PP film surfaces after oxygen

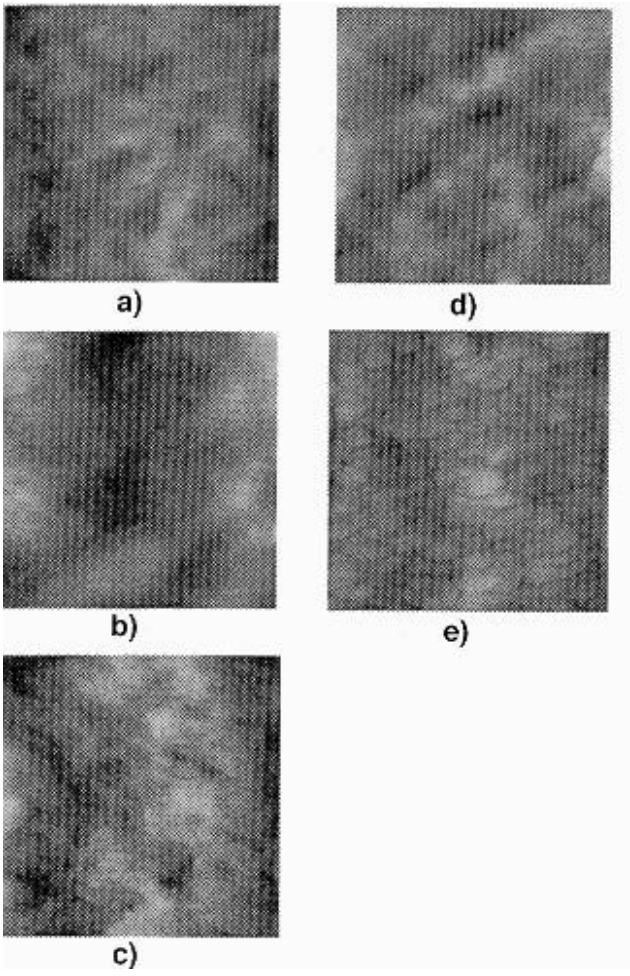


**Figure** 6. AFM image of the kraft pulp surface treated with oxygen plasma for (a) 0, (b) 15, (c) 30, (d) 60, and (e) 90 s. The axis (500 nm × 500 nm) and depth (50 nm) scales are the same for all the images. The gradual increase in the nodule size with the treatment time can be seen.

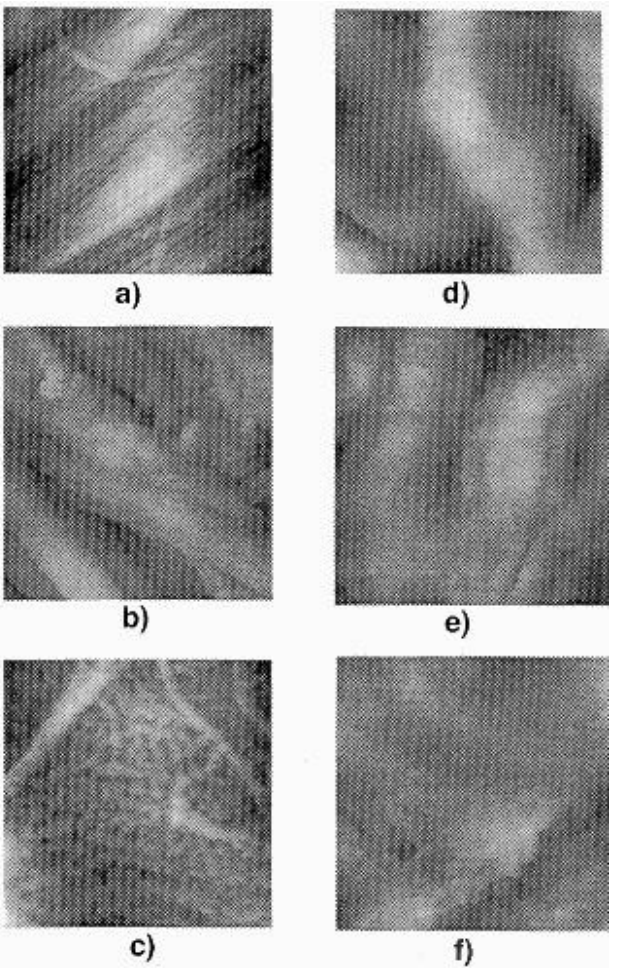


**Figure** 7. Comparison of the effect of oxygen plasma for (a) 0, (b) 30, and (c) 60 s on filter paper and kraft pulp for (d) 0, (e) 30, and (f) 60 s. The axis (2 $\mu$m × 2 $\mu$m) and depth (300 nm) scales are the same for all the images. The formation of the nodular structure becomes prominent at the exposure time of 60 s.

plasma treatment, is clearly visible. In the image, the surface of the wood is covered with nodules. However, this was not the case everywhere on the sample. On some areas, no traces of change were observed. The larger scale analysis of wood surfaces (oxygen plasma treated for 60 s) was performed with SEM microscopy. No sign of plasma treatment was observed in the SEM micrographs.

The surface of kraft pulp used for simulating wood reacts similarly to PP films when exposed to oxygen plasma treatment. Untreated kraft pulp, shown in Figure 6a, has no clear fibril structure but is of a grainlike structure. After a treatment for 15 s, the surface is covered with small nodules of roundish shape, as can be seen in Figure 6b. Treatment for 30 s increases the nodule size, but the macroscopic structure and roughness is still clearly visible as shown in Figure 6c. Further oxygen plasma treatment for 60 and 90 s increases the nodule size, and this also seems to smoothen the surface, as can be noticed in Figure 6d and 6e. There is no point in comparing the roughness values because these greatly depend on the location.

Figure 7a shows the nanofibrillar stucture of a fiber surface in untreated filter paper. Plasma treatment for 30 s did not change the fiber surface, as can be seen in Figure 7b. The microfibrillar structure is still visible. After a plasma treatment for 60 s, the surface of the filter paper changed as shown in Figure 7c. The fibrils are no longer continuous; instead, they seem to consist of roundish structures forming strings of beads, and the shape and orientation of the fibrils are fairly visible. It is not excluded that etching has also taken place. Deeper valleys can be observed between these fibrils. The diameter of the roundish structures is from 100 to 170 nm, which is much larger compared with that of the PP film. The heights measured from cross sections are several tens of nanometers. However, in some cases, the top surfaces of these nodules are flat.

On kraft pulp surface, no distinctive fibrillar structure can be observed. The surface is slightly fragmented as shown in Figure 7d. When treated for 30 s, no significant changes take place (Figure 7e). However, after treatment of 60 s, formation of a nodular-like structure is present, as can be seen in Figure 7f. In addition, etching of the surface is observed.

## Discussion

The SEM technique has commonly been used to study the effects of plasma treatments on polymer surfaces. However, SEM studies have limited depth resolution, which does not enable the detection of morphological features of much less than a micrometer. In addition to this, the high voltage required for larger magnifications with high resolution causes damage to the polymer surface when SEM is used. Damage in terms of the melting of PP film was observed in our experiments carried out using voltages from 15 down to 1 kV. Similar observations on

perfluorinated polymers have been reported by Gengenbach et a1.[22] The development of AFM modes made it possible to adapt this new technique to the topography studies of polymer surfaces with a nanoscale resolution and is therefore likely to give information on the small topographical changes due to plasma treatment. Furthermore, AFM is considered to be a method that is nondestructive to surfaces, especially when the tapping mode is used in the absence of lateral force or shear force.

Comparison of the SEM and AFM images of treated PP film (Figure 2) shows that the surfaces studied with AFM lack the cracks that are prominent in the SEM images. When similar cracks are also seen in the SEM images of untreated PP, it can be concluded that the cracks are due to the analysis technique and not the plasma treatment. The assumption of the origin of the cracks is supported by the SEM micrographs of smaller magnifications on which no cracks of any kind occur. The holes and oriented line structure of the treated PP film seen in Figure 1 (50 $\mu$m × 50 $\mu$m) are likely caused by the manufacturing processes of the film. A similar structure on an untreated PP surface has been reported by Collaud Coen et al.[18]

In this study, the results indicated that the overall roughness of the PP surface decreased slightly with the length of the treatment time (Figure 4). The etching of surfaces (synthetic as well as natural) by plasma treatments has been reported by several authors.[4,27,28] Etching often results in surfaces with reduced overall roughness. In addition, etching is assumed to remove weak boundary layers (e.g., impurities) from the surface. Smoothening of the PP surface due to oxygen plasma has been reported by Collaud Coen et al.;[18] however, no new characteristic changes on the treated PP were observed in that study, while in the present study the treated PP surface became covered with clear nodular structures. The diameter of the nodules observed in this study varied from about 15 to 55 nm. Our findings on untreated PP agree well with those of Viswanathan and Marr,[29] who have worked with polyethylene and reported a granular structure originating from the spherulites of the polymer. The present observation of the increase in the size of the nodules with the treatment time (Figure 3) indicates that etching is not the only explanation for the morphological changes. It is known that the original structure of the polymer surface breaks down and degradation products and active constituents are formed by oxygen plasma.[30,31] Systematic studies carried out in our laboratories indicate that polar C=O and other oxygen-based functionalities are produced on both PP and cellulose surfaces at short treatment times, while etching processes and less favorable chemical changes in terms of adhesion, such as cross-linking, are initiated at longer plasma exposures. The increasing nodule size with the treatment time leads us to believe that sublimation and rearrangement of degradation products originating from the surface of the polymer and/or from possible residues of additives left in the bulk take place on the treated surfaces.

Our findings show that surface changes are due to other processes occurring besides etching. This is in good agreement with the results of some other studies. Droplet-like protrusions have been found on a corona-treated PP surface by Overney et a1.[23] However, there is a 10-fold difference in the diameters of the droplets compared to the nodules observed by us. Overney et a1.[24] proved, by means of friction force and contact-angle measurements, that the protrusions were most likely degradation products which physisorbed on the surface through local melting or sublimation. This assumption was based on the difference in the friction force, showing that the chemical nature of the protrusions differed from that of the surrounding polymer bulk. In addition, the increased friction caused by higher plastic flow on the protrusions was explained as being due to molecules of low molecular weight. AFM images of oxygen-plasma-treated poly(tetrafluoroethylene) by Ryan and Badyal[20] showed that the effect of plasma appears as microroughness superimposed upon the original macroroughness of the polymer. In the case of nitrogen, hydrogen, and argon plasmas, fine globular features were formed on top of the polymer surface by the treatments. However, it was distinctive to this structure that the distribution of the globules was heterogeneous, different from the structure of the treated PP in our study, which was covered by a homogeneous layer of round-shaped features. Among the previous authors, Collaud Coen et al.[18] have found that PP exposed to noble gas plasmas (Ar, He, Xe) undergoes a process that rearranges the surface of the PP and creates a network of macroscopic chains. Oxygen plasma treatment, however, leads to a fairly unchanged topography of the PP film.

Evidence of accumulation of a loosely adhering substance on the PP surface was detected: the fact that the scanning of the PP film using the contact mode modified the surface and that some substance was noticed to stick to the tip in the tapping mode. Based on the observations during this study and the results of the chemical changes referred to above, it can be suggested that plasma treatment forms a layer of low-molecular-weight compounds on the film surface which assumingly adheres poorly to the surface and acts as a failure center in testing. The adhesion values in the peel test showed that the shorter the treatment time, the higher the peel strength values. This result is in good agreement with the study of Young et a1.,[32] who stated that the optimum conditions for oxygen plasma treatment, in terms of adhesion between filter paper and PP film, are low power levels and short treatment times. Based on these results, it may be assumed that the adhesion strength between wood and PP film reaches its peak at the shorter treatment times, when the favorable chemical changes on the surfaces have already taken place, but the weak boundary layer has not yet grown too thick. The results of the adhesion tests support this explanation, showing a 30-120% increase in bonding strength values for the samples treated only 15 s with oxygen plasma, whereas the bonding strength drops to the level of the untreated samples with longer treatment times. Plasma seemed to improve the adhesion properties more when both the PP film and the wood surface were treated, compared to treatment of only one surface. In the study by Carlsson and Ström on the effect of plasma on the adhesion between cellulosic sheet and polyethylene, it has also been stated that the reduction in peel strength observed might be due to the weak boundary layer formed by hydrogen plasma.[33] In the same study, it was found that by removing the weak boundary layer, i.e., the degradation products by extraction, the adhesion properties were regained.

(27) Yasuda, H. *J. Macromol. Sci. Chem. A* **1976,** *10,* 383.
(28) Felix, J.; Carlsson, G.; Gartenholm, P. J. *J. Adhesion Sci. Technol.* **1994,** *8,* 163.
(29) Viswanathan, R.; Marr, W. M. *Langmuir* **1996,** *12,* 1084.
(30) Poncin-Epaillard, F.; Chevet, B.; Brosse, J.-C. *J. Adhesion Sci. Technol.* **1994,** *8,* 455.
(31) Wu, S. *Polymer Interface and Adhesion;* Marcel Dekker Inc., New York, 1982.
(32) Young, R. A.; Denes, F.; Sabharwal, H.; Nielsen, L.; Tu, X. Second Pacific Rim Bio-based Composites Symposium, Vancouver, Canada, 1994.
(33) Carlsson, C. M. G.; Ström, G. *Langmuir* **1991,** *7,* 2492.

Similar growth in the nodule size as on the PP surface occurs also on the lignocellulosic materials (wood, kraft pulp, and filter paper). Individual fibers sticking out from the wood surface, even if sanded, make it difficult to monitor wood by means of AFM. However, comparison of the AFM images of untreated wood (Figure 5a) with the AFM images of treated wood (Figure 5b) showed that plasma treatment in some parts of the wood surface forms nodule-like features similar to those seen on the treated PP. An easier approach toward investigation of the effects of plasma on wood was to study materials of similar composition to wood. Kraft pulp and filter paper were found useful for this purpose. The increasing nodule size and assumed smoothening of the kraft pulp surface with treatment time indicates that deposition/accumulation of substances of some kind, probably degradation products, takes place on the surface. However, it seems unlikely that the changes in the structure of the filter paper are solely attributable to deposition phenomena without etching of the material taking place as well. On the untreated filter paper and to a certain extent on the treated filter paper, an orientated structure due to cellulose fibrils was visible. The fact that nodules caused by plasma follow the alignment of fibrils is an indication of fibril surfaces having potential centers for deposition of the substance formed. In some images of the treated filter paper, there were "bridges" crossing the parallelly aligned bead strings. Kraft pulp is already affected by plasma at the exposure time of 30 s, whereas filter paper did not show any noticeable changes. This indicates that kraft pulp, probably due to the presence of lignin, is likely to be more sensitive to plasma than highly arranged cellulose-rich filter paper. Wood itself behaved pretty much in the same way as filter paper under plasma. Plasma creates affected regions here and there on the wood surface and leaves some areas unaffected in terms of morphology.

## Conclusions

The formation of a nodular surface structure is prominent for the polypropylene and lignocellulosic materials exposed to oxygen plasma. The diameter of the nodules increases with the treatment time. The overall roughness of the surfaces decreases with the treatment time. These phenomena are particularly apparent for the PP surfaces that change from dent- and defect-rich to smooth and more homogeneous surfaces covered with nodules. The topographical changes and observations during the AFM studies indicate that the features of the exposed surfaces are probably caused by different physical and chemical processes (e.g., etching, sublimation of new constituents formed, and/or rearrangement of the surface altered chemically). Adhesion between PP and lignocellulosic materials is slightly improved by the treatment and is related to the exposure time. With oxygen plasma and under the conditions used in this study, the maximum adhesion was reached with the shortest exposure time applied (15 s).

**Acknowledgment.** We thank T. Kuster from the Forest Products Laboratory, Madison, for the SEM work. We gratefully thank Professor P. Hautojärvi from the Laboratory of physics, Helsinki University of Technology, for his interest and support for the work. The work at the University of Wisconsin was mainly funded by a scholarship granted by the Foundation of Technology (Finland) and the Finnish Cultural Foundation.

LA980139B